

A Compressive Sensing Approach for 3D Breast Cancer Microwave Imaging with Magnetic Nanoparticles as Contrast Agent

Martina T. Bevacqua *Student Member, IEEE* and Rosa Scapaticci *Member, IEEE*

Abstract—In microwave breast cancer imaging magnetic nanoparticles have been recently proposed as contrast agent. Due to the non-magnetic nature of human tissues, magnetic nanoparticles make possible the overcoming of some limitations of conventional microwave imaging techniques, thus providing reliable and specific diagnosis of breast cancer. In this paper, a Compressive Sensing inspired inversion technique is introduced for the reconstruction of the magnetic contrast induced within the tumor. The applicability of Compressive Sensing theory is guaranteed by the fact that the underlying inverse scattering problem is linear and the searched magnetic perturbation is sparse. From the numerical analysis, performed in realistic conditions in 3D geometry, it has been pointed out that the adoption of this new tool allows improving resolution and accuracy of the reconstructions, as well as reducing the number of required measurements.

Index Terms—microwave breast cancer imaging, magnetic nanoparticles, compressive sensing, super-resolution, compressed measurements.

I. INTRODUCTION

IN the last years, the evidence that human tissues exhibit different electromagnetic properties at microwaves, depending on their typology and physio-pathological status, has given rise to a huge interest in Microwave Imaging (MWI) for medical applications. The use of non-ionizing radiations and possibly cheap and portable devices represents the main advantage offered by MWI with respect to other medical imaging techniques. In particular, MWI has gained increasing interest in breast cancer diagnostics, as witnessed by the large number of papers published on this topic [1], [2].

However, recent studies on the electric properties of mammary tissues have outlined that the electric contrast between healthy fibroglandular tissues and cancerous ones may be not as high as initially thought [3].

As a consequence, in order to improve sensitivity and specificity of a microwave based diagnostic technique, the

use of contrast agents, able to increase the contrast between fibroglandular healthy tissues and cancerous ones, has been introduced [4]–[6]. In particular, Magnetic Nanoparticles (MNP) has been recently considered [7], [8], since, by exploiting biochemical targeting techniques [9], [10], they present a unique capability of inducing a specific and selective contrast into tumoral tissues. As a matter of fact, the non magnetic nature of human tissues allows to pursue the cancer imaging through the reconstruction of a magnetic contrast, specifically associated to the tumor, embedded into a purely electric scenario.

The feasibility of the technique has been already demonstrated through a wide numerical analysis involving anthropomorphic breast phantoms [11], [12], as well as through preliminary experimental measurements [8].

In particular, in [12] an effective imaging procedure based on the Truncated Singular Value Decomposition (TSVD) has been proposed for the solution of the inverse problem underlying the technique.

Inspired by some peculiar features of MNP enhanced MWI for breast cancer diagnosis, in this paper we exploit the Compressive Sensing (CS) theory [13], [14] for the development of a novel imaging technique. Compressive Sensing represents a new relevant paradigm in signal recovery, especially in inverse scattering problem, as witnessed by recent papers, dealing with the general MWI problem [15]–[17], as well as with medical MWI [18].

Compressive Sensing theory can be applied whenever the problem to be faced is linear and when the unknown is “sparse”, i.e., it can be represented with only few non-zero coefficients in a given basis. Notably, since only a low amount of MNP can actually reach cancerous cells, the inverse scattering problem arising in MNP enhanced MWI can be reliably described through a linear model [7], [12]. In addition, the selective targeting of MNP in the tumor implies that the unknown inclusion is small and localized, so it is intrinsically sparse in the voxel basis.

Starting from these considerations, an *ad hoc* CS algorithm has been tailored for MNP enhanced microwave breast cancer imaging. In particular, the standard CS implementation has been enhanced by exploiting information on the maximum concentration of contrast agent that can be achieved in human tissues [19].

The expected advantages in adopting an inversion technique inspired to CS theory are related to the possibility of achieving high resolution images and reliable reconstructions with a fewer number of antennas, as shown in the preliminary results

This is the post-print version of the following article: M. T. Bevacqua and R. Scapaticci, "A Compressive Sensing Approach for 3D Breast Cancer Microwave Imaging With Magnetic Nanoparticles as Contrast Agent," in IEEE Transactions on Medical Imaging, vol. 35, no. 2, pp. 665-673, Feb. 2016, doi: 10.1109/TMI.2015.2490340. Article has been published in final form at: <https://ieeexplore.ieee.org/document/7297871>.

0278-0062 © 2016 IEEE. Personal use of this material is permitted. Permission from IEEE must be obtained for all other uses, in any current or future media, including reprinting/republishing this material for advertising or promotional purposes, creating new collective works, for resale or redistribution to servers or lists, or reuse of any copyrighted component of this work in other works.

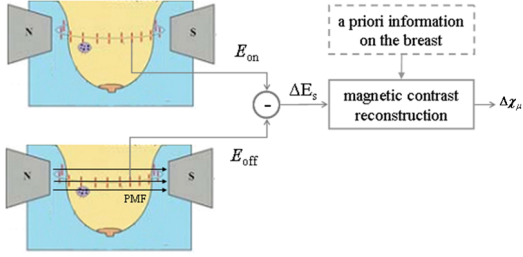


Fig. 1. Conceptual scheme of the MNP enhanced MWI strategy

achieved in 2D geometry and reported in [20]. Both these aspects, jointly with an analysis of the robustness of the imaging procedure against *a priori* information, are addressed in detail in the paper, which is organized as follows. Section II recalls the basics and the mathematical formulation of the MWI technique based on the use of magnetic nanoparticles as contrast agent, while in Section III the Compressive Sensing Theory and its particularization to the application at hand is detailed. In Section IV the test-bed adopted in the following numerical analysis is described. In Section V the effect of unavailable information on the breast under test is assessed and discussed and in Section VI a comparison with the TSVD based inversion is carried out. Finally, in Section VII some conclusions are given.

II. BASICS AND MATHS OF MNP ENHANCED MWI

A key feature of MNP enhanced microwave breast cancer imaging is the adoption of a differential measurement strategy [7], which allows to extract the useful signal, i.e. the signal scattered by the targeted tumor, in a “smart” way. In more details and as schematized in Fig.1, by exploiting the possibility of modulating the magnetic response of MNP when they are exposed to an external polarizing magnetic field (PMF), the technique requires to perform two measurements with two PMFs of different intensities [7], [11]. Since the PMF does not perturb the electric scenario, i.e., the breast under test, the difference of the fields gathered at the two stages of the measurement is actually associated to the magnetic contrast variation into the tumor.

Due to the low magnitude of the magnetic contrast that can be induced within the tumor, it is possible to assume that the induced magnetic anomaly does not perturb the field due to the electric scenario. Hence, the relevant scattering phenomenon can be modeled by means of the distorted Born approximation [21].

Accordingly, by omitting some unessential factors, the generic element $\Delta E_s(r_v, r_m)$ of the $M \times M$ differential scattering matrix (M being the number of adopted probes) is given by [7], [12]:

$$\begin{aligned} \Delta E_s(r_v, r_m) &= \int_{\Omega} \mathbf{G}^{EM}(r_m, r) \Delta\chi_{\mu}(r) \mathbf{H}_i(r, r_v) dr \\ &= \mathcal{L}^{EM} \Delta\chi_{\mu} \quad v, m = 1, \dots, M \end{aligned} \quad (1)$$

wherein Ω denotes the region hosting the breast, r_m denotes the receiving probe’s position and r_v is the position of the

transmitting antenna. $\mathbf{G}^{EM}(r_m, r)$ is the electric-magnetic Green’s function of the reference scenario, i.e., the electric field in r_m generated by an elementary magnetic source in r . $\mathbf{H}_i(r, r_v)$ is the magnetic “incident” field into the electric scenario, i.e., the magnetic field generated by an electric source located in r_v in the point $r \in \Omega$, in presence of the breast, but without any magnetic anomaly. Due to the reciprocity principle, $\mathbf{G}^{EM}(r_m, r) = \mathbf{H}_i^T(r, r_v)$, where the superscript T denotes the transpose matrix. Finally, $\Delta\chi_{\mu}$ represents the differential magnetic contrast, i.e., the susceptibility variation due to the change of the PMF intensity between the two stages of the measurement. As can be seen from (1), the data to unknown relationship is linear, since the operator \mathcal{L}^{EM} does not depend on the unknown $\Delta\chi_{\mu}$ [12].

III. CS INSPIRED APPROACH FOR AN EFFECTIVE RECOVERY

In many traditional approaches, which aim at reconstructing signals from measured data with no loss of information, the well-known Shannon-Nyquist sampling theorem is generally fulfilled. Compressive Sensing Theory [13], [14] overcomes this dogma of signal processing and recovery and allows an accurate retrieval of a given function at a rate significantly below Nyquist and with a number of measurements much lower than the overall number of unknown coefficients.

Let us see in more details the mathematical framework, considering a generic linear problem $y = Ax$, where y is the $M \times 1$ data vector, x is the vector that contains the unknown coefficients of a convenient representation of the function to be retrieved, organized into an N dimensional vector. Finally, A is the $M \times N$ matrix which relates the unknown vector to the data vector. According to CS theory, if the matrix A fulfills given properties (whose discussion is outside of the scope of this paper) and the unknown vector x is sparse, even if M is (much) less than N but it is anyway sufficiently larger than the number of non-null coefficients of x , say S , it is possible to solve the inverse problem by means of the following constrained optimization [22]:

$$\begin{aligned} &\min_x \|x\|_{l_1} \\ &\text{subject to } \|Ax - y\|_{l_2} < \delta \end{aligned} \quad (2)$$

well known as Basis Pursuit denoising (BPDN) or LASSO problem. Numerical analysis of canonical cases suggested that a successful reconstruction is achieved in more than 50% of the cases when $M \geq 4S$, and in more than 90% of the cases when $M \geq 8S$ [13], [14]. Note that in (2) the minimization of the l_1 norm encourages the search of sparse solutions, while the constrain enforces the data consistency. In other words, among all solutions which are consistent with the measured data, one searches the one which is sparse.

A. Cancer Imaging Exploiting CS Theory

In the contrast enhanced MWI technique, recalled in previous section, the non-magnetic nature of human tissues and the capability of MNP of selectively targeting tumoral cells,

allows to assume that the unknown is small and localized, so, intrinsically sparse in the voxel basis.

In addition, the relationship between data and unknowns can be considered linear, as stated in the Section II. As a consequence, CS theory can be exploited as an effective and reliable procedure to accurately image the induced magnetic anomaly.

Accordingly, by exploiting CS theory, the linear problem (1) can be solved by rewriting the optimization in (2) as:

$$\begin{aligned} & \min_{\Delta\chi_\mu} \|\Delta\chi_\mu\|_{l_1} \\ & \text{subject to } \|\mathcal{L}^{EM}\Delta\chi_\mu - \Delta E_s\|_{l_2} < \delta \end{aligned} \quad (3)$$

Notably, the cardinality of the differential data ΔE_s can be (much) smaller than the overall number of voxels into which the investigated domain is discretized, but sufficiently larger than the number of nonzero elements of $\Delta\chi_\mu$.

It is worth saying that the choice of the parameter δ in (3) represents a non-trivial task, as it is the results of a trade-off between the reconstruction accuracy and the feasibility of the optimization task. In fact, it depends on several factors, in particular on the level of required precision, the amount of noise on data and the model error introduced by the estimation of $\mathbf{G}^{EM}(r_m, r)$. In this respect, as one is looking for a solution different from the null vector, a possibility is to set the parameter δ in such a way to fulfill the upper bound $\delta < \|\Delta E_s\|_{l_2}$. Moreover, the larger the expected amount of error and noise on the data, the larger the parameter δ .

In order to exploit all the a priori information about the considered technique, the standard LASSO problem in (3) has been enhanced by considering a further constraint, i.e.:

$$|\Delta\chi_\mu| \leq |\Delta\chi_\mu|_{MAX} \quad (4)$$

In fact, the maximum concentration of MNP which can be targeted into human tissues is known from biochemical studies and, for this reason, it is reasonable assuming also the maximum amplitude of the magnetic contrast $|\Delta\chi_\mu|_{MAX}$ induced in the tumor [19], [23].

The addition of the constrain (4) represents a kind of tailored implementation of CS for MNP enhanced microwave breast cancer imaging and, as observed in some numerical tests reported in the following, the optimization problem greatly benefits of this additional constraint.

IV. DESCRIPTION OF THE TEST BED AND VALIDATION OF THE PROPOSED APPROACH

The performance of the imaging strategy herein proposed have been assessed with respect to two different anthropomorphic breast phantoms, derived from magnetic resonance images and taken from the Wisconsin University Repository [24]. In particular, two phantom have been taken into account:

- a heterogeneously dense breast (ID: 070604PA2), denoted in the following as *Ph1*.
- a scattered fibroglandular breast (ID: 012204), characterized by a high percentage of adipose tissue and denoted as *Ph2*.

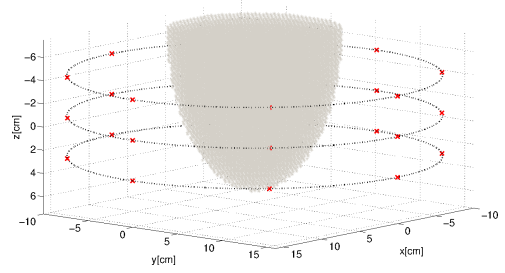


Fig. 2. Measurement configuration

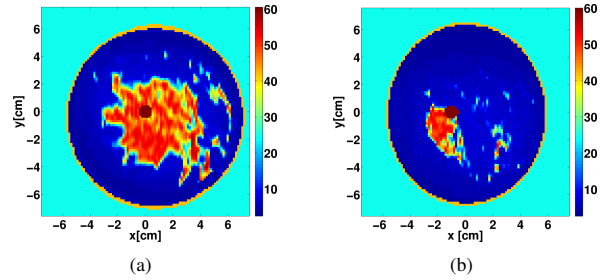


Fig. 3. Transversal slices of the permittivity maps across the tumor for the two considered phantoms: (a) *Ph1*; (b) *Ph2*.

In both cases the breast is immersed in a homogeneous lossless matching medium, whose relative permittivity is $\epsilon_b = 25$.

The adopted measurement configuration is depicted in Fig. 2 and it consists of a 3 rings array of z-directed elementary dipoles working both in transmitting and receiving mode at a fixed frequency of 2 GHz. The array is centered with respect to the imaging domain and each ring, of radius 16 cm and containing 8 probes, is 3.5 cm far from the other one. In such a way the total number of independent measurements is equal to 300 [25].

In all the following examples, the tumor has been modeled as a spherical inclusion of 1 cm in size, having same electric features of the fibroglandular tissue ($\epsilon_{tum} = 60$, $\sigma_{tum} = 0.7$). In *Ph1* the inclusion is positioned at $(0\text{cm}; 0\text{cm}; 1.2\text{cm})$, in fibroglandular tissue, while in *Ph2* it lies at $(0\text{cm}; -1\text{cm}; 0\text{cm})$, across fatty and fibroglandular tissues. The transverse slices of the corresponding permittivity profiles, cutting the center of the tumors are shown in Fig.3. A variation of the magnetic contrast between the two stages of the measurement of $|\Delta\chi_\mu| = 0.0094$ has been considered. Note that, according to the experimental results reported in [11], [23], this differential magnetic contrast corresponds to a realistic MNP concentration of about $12\text{mg}/\text{cm}^3$. For this consideration, $|\Delta\chi_\mu|_{MAX}$ is chosen equal to 0.01.

All the data for the described phantoms have been simulated by using a full-wave forward solver based on a conjugate gradient FFT implementation of the method of moments. Moreover, an accurate discretization of the electromagnetic fields and a faithful description of the tissue's morphology are considered. An additive gaussian noise with $SNR = 20$ dB on the scattered field is considered.

As a first validation of the proposed imaging method, we have assessed the role played by the constrain in (4) on the

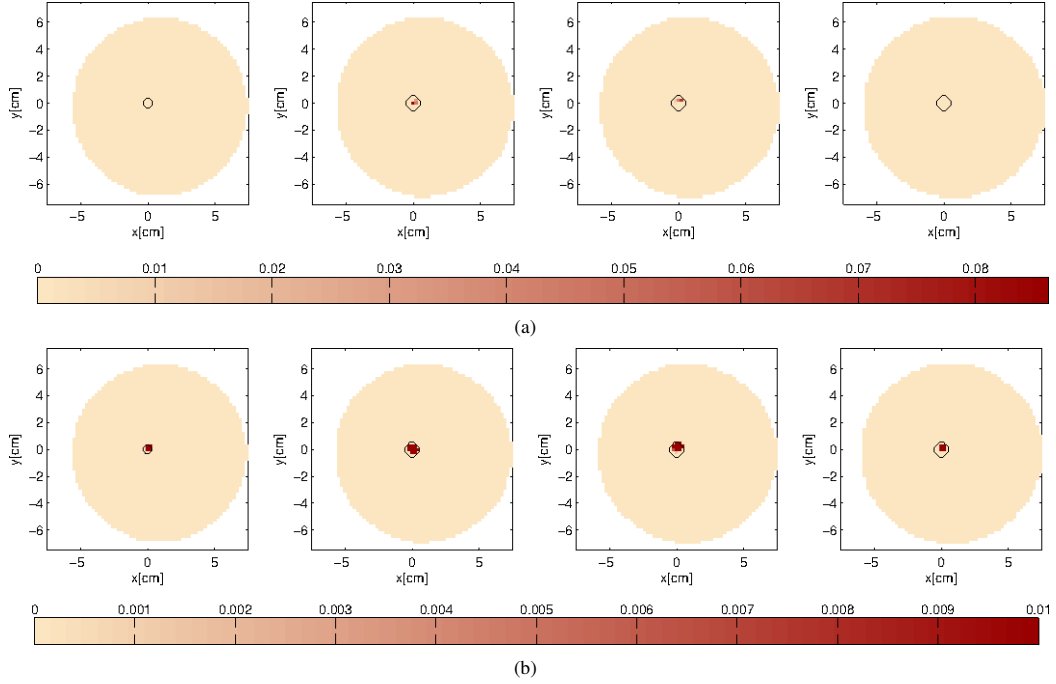


Fig. 4. Transversal slices of the retrieved absolute value of the induced magnetic contrast ($Ph1$): (a) via standard CS implementation (b) by means of the proposed method. The black line indicates the actual contour of the tumor

maximum amplitude of the unknown magnetic contrast. To this end, we have considered the example concerning $Ph1$ and compared the results obtained by applying a standard CS implementation and those provided by the proposed method. As shown in Fig.4, the presence of the additional constraint in (4) is crucial to obtain a reliable reconstruction of the inclusion volume. In fact, the standard CS, while providing an effective detection and localization of the tumor, does not allow an accurate identification of the tissues affected by the malignancy¹. Note also that in Fig.4a, the maximum retrieved magnetic contrast (absolute value) is greatly overestimated.

V. ANALYSIS OF ROBUSTNESS AGAINST *a priori* INFORMATION ON THE BREAST UNDER TEST

The relationship between the differential scattered field and the induced magnetic contrast, reported in (1), while being linear, depends on the electric properties of the breast under test through the electric-magnetic Green's function \mathbf{G}^{EM} or equivalently through the magnetic field \mathbf{H}_s . In practice, the exact knowledge of the electric scenario (and of the corresponding magnetic field inside it) is not available. Accordingly, a more or less accurate reference scenario is usually considered [12]. In this section the role played by *a priori* information on the breast under test on the proposed CS algorithm is evaluated.

In this analysis, both $Ph1$ and $Ph2$ have been taken into account and three reference scenarios have been assumed, that is:

¹In this first validation the exact knowledge of the electric features of the breast is assumed.

- exact breast, that is the ideal (not realistic) case in which the breast under test is completely characterized. The results obtained with this reference scenario represent a sort of best achievable ones;
- accurate representation of the breast, in which the breast morphology is supposed exactly known, while the electric properties of the adipose and fibro-glandular tissues are supposed to be constant and set according to the average values provided in [3].
- empty system filled by a medium having the same properties as the background, i.e., the coupling liquid. This is the case in which no *a priori* information on the breast is assumed.

As mentioned in the Section III-A, the error model, that is the fidelity of the reference scenario with the true one, affects the choice of the δ parameter. In general, the higher is the error model we are committing, the higher is δ . When the exact breast is assumed, δ only depends on the level of noise on data. In this paper we have assumed $\delta = 0.1\|\Delta E_s\|$, when the exact breast is assumed, $\delta = 0.4\|\Delta E_s\|$, when the approximated breast is considered and $\delta = 0.8\|\Delta E_s\|$ when no *a priori* information is available. Corresponding reconstructions for both $Ph1$ and $Ph2$ are reported in Fig.5.

As can be seen, also with no *a priori* information on the breast under test CS is able to provide accurate results, both in terms of detection and of imaging. In addition, in order to quantitatively assess the quality of the reconstructions, the total reconstructed magnetic polarizability has been evaluated. This quantity is estimated by computing the integral of the reconstructed magnetic contrast on the overall imaging domain

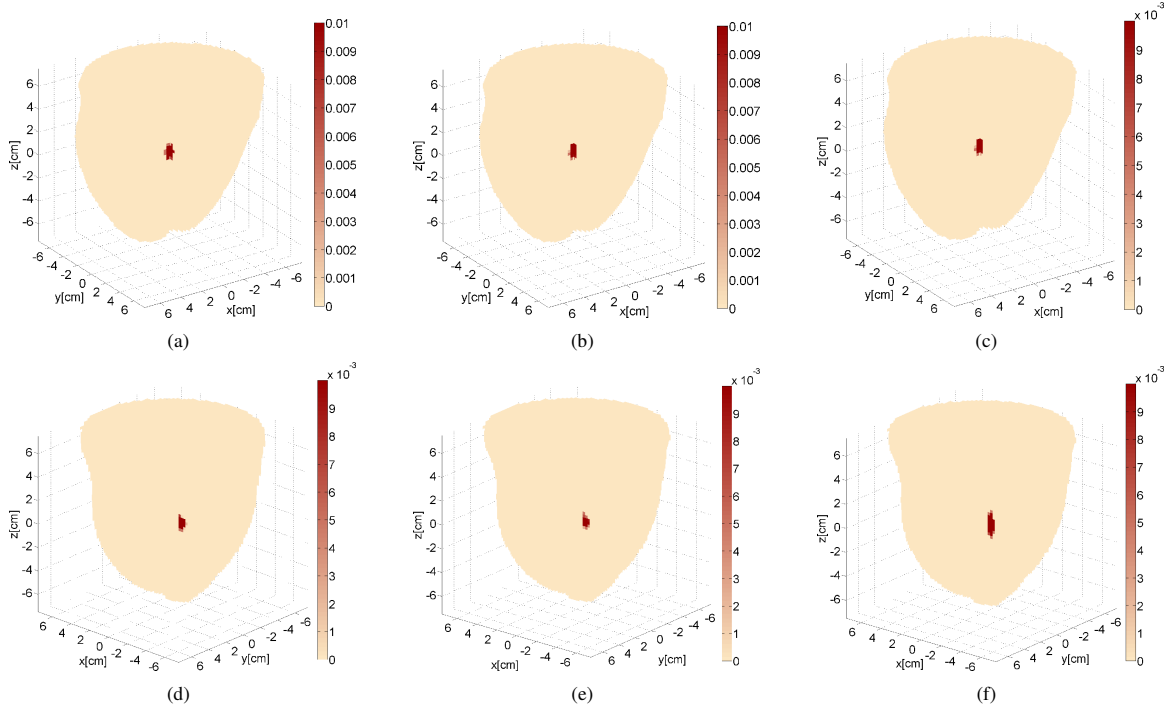


Fig. 5. 3D Reconstructions of the absolute value of the induced magnetic contrast. (a) *Ph1* and exact breast as reference scenario; (b) *Ph1* and accurate reference breast; (c) *Ph1* and background as reference profile; (d), (e) and (f) same as (a), (b) and (c) but for *Ph2*.

[12]. For the considered examples, the values of the retrieved magnetic polarizability are reported in Table I. As can be seen, in all cases the estimated values are close to the actual polarizability value (4.8 mm^3 , obtained by multiplying the actual tumor's volume times the magnetic contrast $|\Delta\chi_\mu| = 0.0094$ induced by the assumed MNP concentration). The correct estimation of the magnetic polarizability is of interest because it allows appreciating the total amount of nanoparticles which has been targeted, related to the tumor's size and to the achieved MNP concentration [7]. It is worth recalling that the TSVD based inversion fails in retrieving the actual magnetic polarizability when no *a priori* information on the breast is assumed [12].

VI. CS INSPIRED IMAGING STRATEGY VS TSVD

As previously discussed, provided that the problem to be solved is linear and that the searched unknown is sparse, the use of CS theory allows, from one hand, a significantly reduction of the number of measurements to perform in order to get reliable results, and on the other hand, fixing the number of performed measurements, to retrieve high resolution reconstructions.

TABLE I
RETRIEVED POLARIZABILITY [mm^3]

breast	exact RES	accurate RES	background RES
<i>ph1</i>	3.96	3.27	6.56
<i>ph2</i>	3.97	3.14	5.86

In the following, both these aspects will be considered and the achievable performance of the CS inspired algorithm will be compared to those obtained for a commonly used approach to solve inverse linear and ill posed inverse problem, that is the Truncated Singular Value Decomposition (TSVD) procedure [21], previously considered in [12]. Moreover, by relying on the results reported in previous Section, no *a priori* information will be considered.

A. Reducing the number of measurements

In microwave medical imaging, the minimization of the number of adopted probes plays a crucial role. As a matter of fact, this would allow to minimize costs and dimensions of the system, as well as measurement time. Moreover, reducing the system complexity has a particular relevance for MNP enhanced MWI, where data are acquired through a two-stage differential measurement process. In fact, the acquisition has to be performed quickly enough to avoid any variation of the electric scenario between the two stages and this is obviously a challenging goal when the number of probes is larger and larger.

In the following, the possibility of reducing the number of probes while preserving the accuracy of the tumor reconstruction has been assessed. In particular breast *Ph2* has been considered and a measurement configuration constituted by only 12 probes on 3 rings (4 probes per ring, arranged as depicted in Fig. 6a) is adopted. In this way, the total number of independent measurements is equal to 78 [25].

Results reported in Fig.6 demonstrate that, opposite to TSVD approach (reported in panel (c) of Fig.6), CS (Fig.6b)

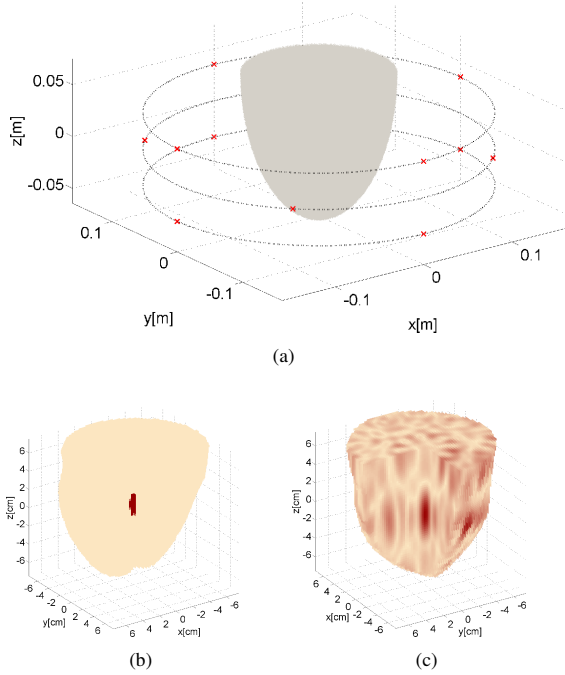


Fig. 6. Normalized 3D Reconstructions of the absolute value of the induced magnetic contrast exploiting 12 probing and receiving antennas and background as reference profile. (a) New measurements configuration; reconstruction via CS and (b) via TSVD.

allows a reliable and accurate recovery also with very few antennas.

B. Super-resolution imaging

In cancer imaging, the possibility of recovering with a high resolution the boundaries of the cancer is extremely important. As a matter of fact, the shape of the inclusion is associated to the degree of malignancy of the cancer: the more irregular is the border the more aggressive is the disease. Accordingly, in order to appreciate the potential of the method in providing super-resolution images, we have analyzed the case in which the tumor is modeled as an irregular structure. In particular, phantom *Ph1* and the measurement configuration reported in Fig.2 have been considered. Again, for the sake of comparison, TSVD inversion has been also performed. Corresponding results are shown in Fig.7. In panels (a) and (b) are reported the 3D reconstructions obtained via CS and TSVD, respectively (this latter cut at -3 dB). Panels (c) and (d) show the reconstructed transversal slices in which the tumor is located, and the actual contour of the cancer, which is superimposed as a black line. Such reconstructions clearly demonstrate that CS outperforms TSVD as far as resolution is concerned, as it allows to appreciate with a satisfactory accuracy the irregular shape of the cancer, not possible from TSVD images.

VII. CONCLUSIONS AND DISCUSSION

Magnetic nanoparticles have been recently proposed as contrast agent in breast cancer MWI. Once properly functionalized, MNP are able to concentrate in cancerous cells in a

selective way, hence their adoption allows to face the cancer imaging as the reconstruction of a magnetic contrast into a purely electric scenario.

In such a framework, the adoption of an effective and robust imaging algorithm represents a key-point for the an accurate and specific breast cancer diagnosis.

By relying on the fact that in MNP enhanced breast cancer MWI the problem to be solved is linear, and the unknown magnetic contrast is small and well localized (and so intrinsically sparse), in this paper we have proposed a novel imaging procedure inspired to Compressive Sensing theory. In particular, an *ad hoc* CS algorithm has been developed exploiting the knowledge of the maximum concentration of MNP that can be targeted in human tissues.

The preliminary results obtained in the 2D case [20] have encouraged us to further investigate the potentiality of the CS approach in the framework in 3D geometry, as well as assess the robustness of the imaging procedure with respect to the lack of *a priori* information of the breast under test in order to assess its diagnostic performance in realistic conditions.

The numerical results have shown that, provided that the parameter δ is properly chosen, one can accurately image cancerous inclusions also in absence of any patient-specific information on the breast under test. On the other hand, an even rough knowledge of the electric properties of the breast can improve the CS results and this pushes towards a parallel line of research, that is to exploit quantitative MWI techniques [26], [27] to retrieve the (approximate) distribution of the electric properties of patient's breast.

As far as the comparison between the proposed CS strategy and TSVD imaging procedure (so far adopted in [12]) is concerned, the main results of the analysis carried out in this paper can be summarized as follows:

- 1- Opposite to the TSVD procedure, the CS inspired approach allows the achievement of reliable results with low amount of data, involving a significant reduction of the number of antennas, thus a significant reduction of the measurement apparatus complexity;
- 2- CS allows a more accurate imaging of the cancer in term of achievable resolution. In particular, the possibility to obtain a sort of super-resolution is a crucial feature of the proposed imaging technique, as the shape of the inclusion is associated to the degree of malignancy of the cancer.

Beside these interesting advantages, it is worth mentioning that the proposed inversion technique involves the solution of a constrained optimization problem, which relies on an iterative procedure, so not very computationally efficient. This represents a drawback with respect to quasi real time procedures, like TSVD. On the other hand, a possible way to meet both accuracy and efficiency, could be the development of a step-wise procedure, in which the TSVD is firstly adopted to detect and localize the tumor, while the CS is explored to refine the reconstruction and pursue a high resolution image. Note that, the first step can be performed in quasi real-time, since the computationally intensive part of the algorithm (which involves the building and the SVD computation of the scattering operator) can be moved offline [12]. Then, once the tumor is detected and localized, it is possible to reduce the

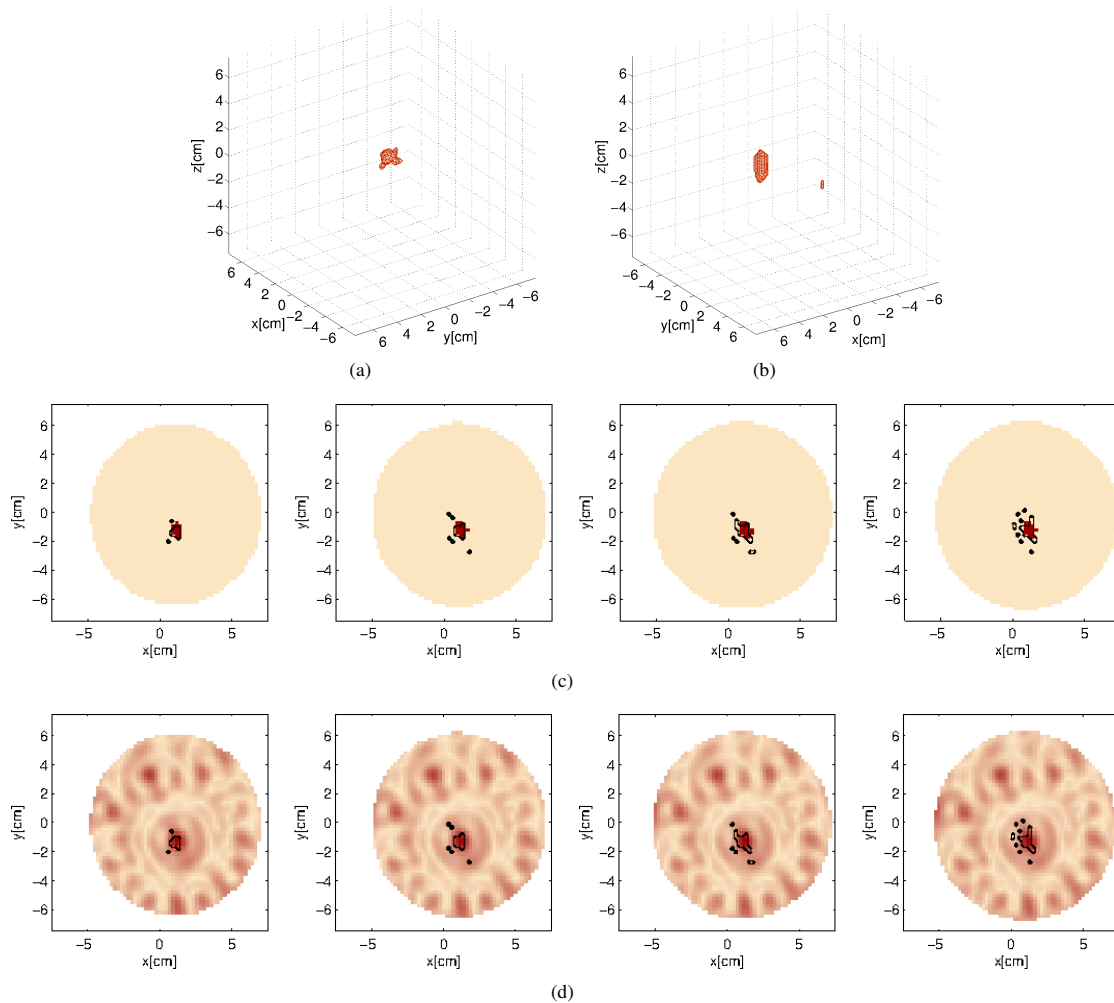


Fig. 7. Normalized 3D Reconstructions of the absolute value of the induced magnetic contrast via CS(a) and via TSVD(b). Transversal slices (across the tumor) of the normalized amplitude of the reconstructed differential magnetic contrast obtained via CS(c) and via TSVD(d).

imaging domain in the CS step and this allows a considerable reduction of the computational burden.

ACKNOWLEDGMENT

The authors want to acknowledge Prof. Ovidio M. Bucci, Prof. Tommaso Isernia and Dr Lorenzo Crocco for the fruitful discussions, which inspired the writing of this paper.

REFERENCES

- [1] T. M. Grzegorzcyk, P. M. Meaney, P. A. Kaufman, R. M. di Florio-Alexander, and K. D. Paulsen, "Fast 3-D tomographic microwave imaging for breast cancer detection," *IEEE Tran. on Med. Imaging*, vol. 31, no. 8, pp. 1584-1592, Aug. 2012.
- [2] J. Bourqui, J. M. Sill, and E. C. Fear, "A prototype system for measuring microwave frequency reflections from the breast," *Int. J. Biomed. Imag.*, vol. 12p, 2012, Art. ID 851234.
- [3] M. Lazebnik et al., "A large-scale study of the ultra wideband microwave dielectric properties of normal, benign and malignant breast tissue obtained from cancer surgeries," *Phys. Med. Biol.*, vol. 52, pp.6093-6115, 2007.
- [4] J. Shea, P. Kosmas, B. V. Veen, and S. Hagness, "Contrast enhanced microwave imaging of breast tumors: A computational study using 3D realistic numerical phantoms," *Inverse Problems*, vol. 26, no. 7, pp.1-22, 2010.
- [5] A. Mashal, B. Sitharaman, X. Li, P. Avti, A. Sahakian, J. Booske, and S. Hagness, "Toward carbon-nanotube-based theranostic agents for microwave detection and treatment of breast cancer: Enhanced dielectric and heating response of tissues-mimicking materials," *IEEE Trans. Biomed. Eng.*, vol. 57, no. 8, pp.1831-1834, Aug. 2010.
- [6] Y. Chen, I. J. Craddock, and P. Kosmas, "Feasibility study of lesion classification via contrast-agent-aided UWB breast imaging," *IEEE Trans. Biomed. Eng.*, vol. 57, no. 5, pp. 1003-1007, May 2010.
- [7] G. Bellizzi, O. M. Bucci, I. Catapano, "Microwave Cancer Imaging Exploiting Magnetic Nanoparticles as Contrast Agent", *IEEE Trans. On Biomed. Eng.*, vol. 58, no.9, pp.2528-2536, Sept. 2011.
- [8] M. Helbig, J. Sachs, F. Tansi, I. Hilger, "Experimental Feasibility Study of Contrast Agent Enhanced UWB Breast Imaging by Means of M-Sequence Sensor Systems", *Proc. of EuCAP2014*, 2014.
- [9] C. Leuschner, C. Kumar, W. Hansel, W. Soboyejo, J. Zhou, and J. Hormes, "LHRH-conjugated magnetic iron oxide nanoparticles for detection of breast cancer metastases," *Breast Cancer Res. Treatment*, vol. 99, pp.163-176, 2006.
- [10] J. Park, G. vonMaltzahn, L. Zhang, A. Derfus, D. Simberg, T. J. Harris, E. Ruoslahti, S. Bhatia, and M. Sailor, "Systematic surface engineering of magnetic nanoworms for in vivo tumor targeting," *Small*, vol. 5, no. 6, pp. 694-700, 2009.

- [11] O. M. Bucci, G. Bellizzi, I. Catapano, L. Crocco, R. Scapaticci, "MNP enhanced microwave breast cancer imaging: measurement constraints and achievable performance", *IEEE Antennas and Wireless Propagat. Lett.*, vol. 11, pp. 1630-1633, 2012.
- [12] R. Scapaticci, G. Bellizzi, I. Catapano, L. Crocco, O.M. Bucci, "An Effective Procedure for MNP-Enhanced Breast Cancer Microwave Imaging", *Trans. on Biomed. Eng.*, vol. 61, pp. 1071-1079, 2014.
- [13] D. Donoho, "Compressed sensing," *IEEE Trans. Inf. Theory*, vol. 52, n. 4, pp. 1289-1306, 2006.
- [14] R. G. Baraniuk, Compressive sampling, *IEEE Signal Process. Mag.*, vol. 24, no.4, pp. 118-124, Jul. 2007.
- [15] E. A. Marengo , R. D. Hernandez , Y. R. Citron , F. K. Gruber , M. Zambrano and H. Lev-Ari "Compressive sensing for inverse scattering", Proc. XXIX URSI Gen. Assem., 2008.
- [16] Bevacqua, M.; Crocco, L.; Di Donato, L.; Isernia, T., "Microwave Imaging of Non-Weak Targets Via Compressive Sensing and Virtual Experiments," *Antennas and Wireless Propagation Letters, IEEE* , in press.
- [17] Bevacqua, M.; Isernia, T.; Crocco, L.; Di Donato, L., "A (CS)² approach to inverse scattering," *Antenna Measurements & Applications (CAMA), 2014 IEEE Conference on* , vol., no., pp.1,3, 16-19 Nov. 2014.
- [18] Azghani, M.; Kosmas, P.; Marvasti, F., "Microwave Medical Imaging Based on Sparsity and an Iterative Method With Adaptive Thresholding," *Medical Imaging, IEEE Transactions on* , vol.34, no.2, pp. 357-365, Feb. 2015.
- [19] L. Josephson, C. H. Tung, A. Moore, and R. Weissleder, High efficiency intracellular magnetic labeling with novel superparamagnetic-Tat peptide conjugates, *Bioconjug. Chem.*, vol.10, pp.186-191, 1999.
- [20] M. Bevacqua, R. Scapaticci, "Magnetic Nanoparticles Enhanced Breast Cancer Microwave Imaging Via Compressive Sensing", *Proc. of the 9-th European Conference on Antennas and Propagation (EuCAP)*, Apr. 2015.
- [21] M. Bertero. Linear inverse and ill-posed problems. *Adv. Electron. Phys.*, 75:1120, 1989.
- [22] S. Chen, D. M. Donoho, D. Saunders, "Atomic decomposition by basis pursuit", *SIAM J. Sci. Comput.*, vol. 20, n. 1, pp. 33-61, 1999.
- [23] G. Bellizzi, O.M. Bucci, "A novel measurement technique for the broad characterization of diluted water ferrofluids for biomedical applications", *IEEE Trans. on Magnetism*, vol. 49, issue 6, pp. 2903-2912, 2013.
- [24] E. Zastrow, S.K. Davis, M. Lazebnik, F. Kelcz, B.D. Van Veem, and S.C. Hagness, "Database of 3D Grid-Based Numerical Breast Phantom for use in Computational Electromagnetics Simulations", *IEEE Trans. Biomed. Eng.*, vol. 55, no.12, pp. 2792-2800, 2008.
- [25] O. M. Bucci and T. Isernia, Electromagnetic inverse scattering: retrievable information and measurement strategies, *Radio Sci.*, 32: 21232138, 1997.
- [26] D.W. Winters, J.D. Shea, P. Kosmas, B.D. Van Veen, and S. C. Hagness, "Three-dimensional microwave breast imaging: Dispersive dielectric properties estimation using patient-specific basis functions", *IEEE Trans. on Medical Imaging*, vol.28, no. 7, pp.969-981, 2009.
- [27] R. Scapaticci, P. Kosmas, L. Crocco, "Wavelet-Based Regularization for Robust Microwave Imaging in Medical Applications," *IEEE Trans. on Biomedical Engineering*, vol.62, no.4, pp.1195-1202, April 2015